Reply to the comments by Karine Deboudt

We appreciate the valuable comments.

Comment (1) Several samples were collected, but considering the technical difficulties for sample preparation, one sample was only studied for its mineralogical properties and internal structures (collected the 15 July 2005 at 9:33). How was it chosen among all samples? Which impaction stages were selected? Why? What was the PM2.5 concentration during sampling? It should be more precisely exposed in the "sample and methods" part.

Reply (1) The sample was chosen due to its closeness to the campaign average in terms of composition and trajectories. Particles were analyzed from the super-micron impaction stages, as they are most complex with respect to optical properties. We have added the corresponding description to the manuscript. Mass concentrations are unfortunately not available for the campaign, but AOT data from aerosol and WDCA shows that the sample was taken during a medium AOT.

Changes in manuscript (1) Corresponding information is provided in the supplement Fig. 1.

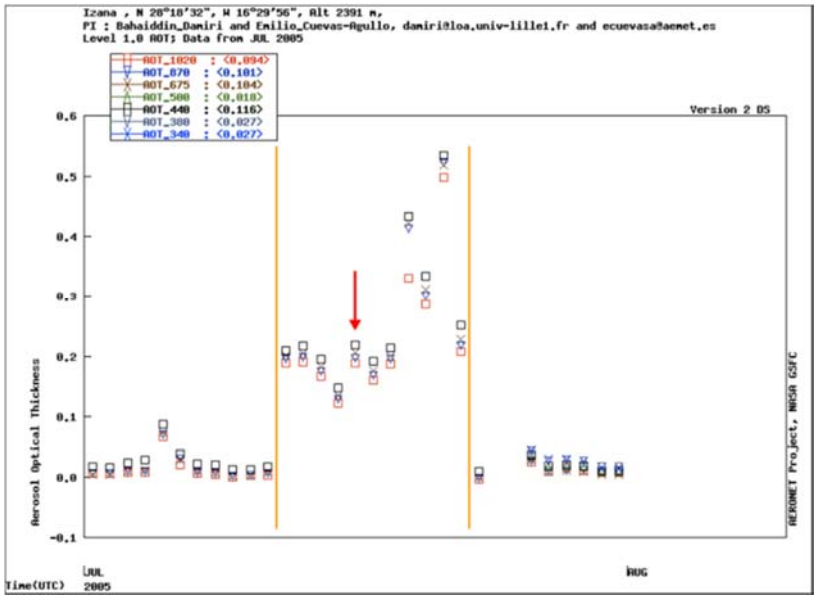

Supplement Fig. 1: Aerosol Robotic Network aerosol optical thickness for Izana, July 2005. Begin and end of the July dust period is marked by orange bars, the sampling day is indicated by a red arrow. Figure created by http://aeronet.gsfc.nasa.gov/cgi-bin/bamgomas_interactive on September 6th, 2016.

We changed the first paragraph of the section 2 Samples and methods to **"**Dust samples used in this study collected from the top of the tower building of the meteorological observatory of Izaña, Tenerife, Spain (28° 18' 33.8" N, 16° 29' 56.9" W, 2395 m a.s.l.). Details on the procedure and location can be found in Kandler et al. (2007). Particles were collected with a cascade impactor on carbon adhesive, with nominal stage size ranges of > 2.6 µm, 0.9–2.6 µm, and 0.1–0.9 µm (50 % efficiency cut-off aerodynamical particle diameter), of which the stages with > 0.9 µm were used for analysis. All samples were stored in a desiccator under dry conditions prior to analysis. The sample analyzed in the present work was collected during a 10 min period on 15 July 2005 at 09:33 h (UTC). It was selected as best-representing the campaign to achieve the greatest atmospheric relevance. Its composition is close to the mean campaign composition (cf. Kandler et al., 2007, Fig. 8), and the corresponding transport trajectory is central in the observed trajectory field (Fig. 1 and Kandler et al., 2007, Fig. 9). According to AERONET aerosol optical thickness data (Supplement Fig. 1), the concentration on the sampling day was also close to the average of the dust event lasting from July 12 to July 22, 2005.

Analysis was limited to particles with diameter < 5 μm, as too few larger ones were available**"**

SEM-EDXS results of two impact stages were added to Table 1.

Table 1. Mineral number % of Saharan dust based on SEM-EDXS analyses of single particles.

Size	No. of particle	Total clay minerals	ISCMs*	Ka	Ch	Bt	Q	P	Kf	Am	Ca	D	Fe	Ti	Gy	Sp	Ap
Saharan dust, Tenerife (This study)																	
0.9-2.5 μm	*n*=1191	1005	868	131	6	0	105	21	17	1	12	5	8	8	9	0	0
	%	84.4	72.9	11.0	0.5	0.0	8.8	1.8	1.4	0.1	1.0	0.4	0.7	0.7	0.8	0.0	0.0
> 2.5 μm	*n*=435	314	260	45	8	1	59	23	17	1	9	1	3	2	4	1	1
	%	72.7	60.2	10.4	1.9	0.2	13.7	5.3	3.9	0.2	2.1	0.2	0.7	0.5	0.9	0.2	0.2
Total	*n*=1626	1319	1128	176	14	1	164	44	34	2	21	6	11	10	13	1	1
	%	81.1	69.4	10.8	0.9	0.1	10.1	2.7	2.1	0.1	1.3	0.4	0.7	0.6	0.8	0.1	0.1
Asian dust, Korea (Jeong and Achterberg, 2014)**																	
%		56.1	48.4	1.8	3.9	2.1	18.7	10.5	4.0	0.7	6.5	1.0	1.2	0.2	0.8	0.2	0.2

*ISCM=illite-smectite series clay minerals, Ka=kaolinite, Ch=chlorite, Bt=biotite, Q=quartz, P=plagioclase, Kf=K-feldspar, Am=amphibole, Ca=calcite, D=dolomite, Fe=iron (hydr)oxide, Ti=Ti oxide, Gy=gypsum, Sp=sphene, Ap=apatite.

** Average value of the SEM-EDXS results from three Asian dust samples presented in Jeong and Achterberg (2014). Vaules are slightly differernt from those in Jeong and Achterberg (2014) by the change of mineral species considered for quantification.

Comment (2) Criteria used for the identification of predominant minerals both from EDX data and electron diffraction/lattice fringe imaging should be presented in supporting information.

Reply and Changes in the manuscript (2) The procedures of mineral identification using EDXS, lattice fringe imaging, and electron diffraction are now provided in **supplement information** as attached at the end of this letter.

Comment (3) In the section 3.1, the relative abundance of clay mineral particles obtained from SEM-EDXS data (Table 1) for the Tenerife sample is directly compared with the total clay content (in wt%?) determined by XRD for a Cape Verde sample, but they are two different physical parameters. This point should be clarified.

Reply (3) Both data are incomplete because of the lack of either XRD or SEM-EDXS data. This is caused by the nonavailability of samples suitable for XRD in Tenerife and SEM-EDXS single particle analysis in Cape Verde (sampling campaigns were done many years ago).

Changes in the manuscript (3) We deleted the comparison of Tenerife SEM-EDXS data to Cape Verde XRD data.

Comment (4) In the section 3.3, the volume of iron (hydr)oxides in the dust particles is estimated. Two dimensions of the iron grains in dust are obtained from the bright-field TEM images, but how is measured the third dimension, notably for internal grains? From EDX maps? It should be explained.

Reply (4) The third dimension of iron (hydr)oxides was not measured. The percentage was derived by measuring the relative area of the iron (hydr)oxides from TEM images by counting pixel using the lasso tool and histogram of ADOBE PHOTOSHOP. In fact, the FIB slices cannot be used to measure the volume of mineral grains included in the dust particles because large portion of the included grains were commonly removed by the FIB work. In addition, we do not have any method to directly measure the volume of included submicron to nano-sized grains yet. However, the area% of included grains approximates the volume% (Vepraskas and Wilson, 2008, Soil Micromorphology: concepts, techniques, and applications, in: Methods of Soil Analysis, Part 5). Although the third dimension of iron (hydr)oxides could not be measured from the FIB slices, the area% of iron (hydr)oxide grains in a dust particle approximates their volume %. If the iron (hydr)oxide grains imaged by TEM are the only iron (hydr)oxides included in the dust particle, the volume of host particle would be enormously larger than the volume of tiny iron (hydr)oxides in comparison to corresponding areas because volume is proportional to the cube of the diameter. However, the FIB slices expose a cross section of iron (hydr)oxide grain which was randomly selected from many iron (hydr)oxide grains dispersed through the dust particle. Thus, area% approximates volume%. We would like to keep volume%.

Changes in the manuscript (4) We inserted following sentences: "Although the third dimension could not be measured, the area% of iron (hydr)oxide grains approximates volume% because tiny iron (hydr)oxide grains had been randomly dispersed through the dust particle (Vepraskas and Wilson, 2008)."

Comment (5) The section "3.5 Shape of dust particles" notably presents the methodology to measure the total particle volume, so it should be inserted before the part 3.3 in which particle volumes are presented and also discussed (sup Table 1).

Reply (5) We are interested in the volume of iron (hydr)oxides. The area of iron (hydr)oxides was measured by counting pixel using the lasso tool and histogram of ADOBE PHOTOSHOP. We did not measure their *a*, *b*, and *c* dimensions.

Changes in the manuscript (5) We would like to keep part 3.5.

Technical correction (6) (Avila et al., 1997) is cited in the introduction, but (Avila et al., 1996) is listed in the bibliography.
Reply and Changes in the manuscript (6) The bibliography was corrected to 1997.

Technical correction (7) (Conny, 2013) is cited in the introduction, but it is not among the listed references.
Reply and Changes in the manuscript (7) Conny (2013) was added to the list.

Technical correction (8) Figure 1: What is the level high of the arrival air masses for the backward trajectory calculations by HYSPLIT? It should be mentioned in the Figure caption.
Reply and Changes in the manuscript (8) "Izana" was changed to Izana (2400 m asl.).

Technical correction (9) Figure 2: The meaning of yellow lines is given two times in the Figure caption.
Reply and Changes in the manuscript (9) One of the repeated sentences was deleted.

Supplement Information – Mineral identification

Minerals have their own crystal structures and chemical compositions. Thus, mineral identification using TEM is based on the lattice-fringe imaging and electron diffraction providing structural information and EDXS providing chemical information. Precise identification of all the minerals in the FIB slice to the species level is practically impossible because of beam damage, high vacuum, lower reliability of lattice fringes/electron diffraction data in comparison with XRD, and enormous time required.

TEM identification of nonphyllosilicate minerals

The identification of quartz, K-feldspar, plagioclase, calcite, amphibole, dolomite, titanite, apatite, and gypsum was straightforward based on their characteristic EDX spectra (Fig. S1). Although we could not identify mineral species of K-feldspar (sanidine, orthoclase, microcline), plagioclase (albite, oligoclase, andesine...), and amphibole (tremolite, actinolite, hornblende...) using time-consuming complex operation, the purpose of current mineral dust research was satisfied by grouping similar mineral species. Silica phase of the mineral dust from desert was almost quartz, consistent with XRD although few amorphous silica was identified by electron diffraction.

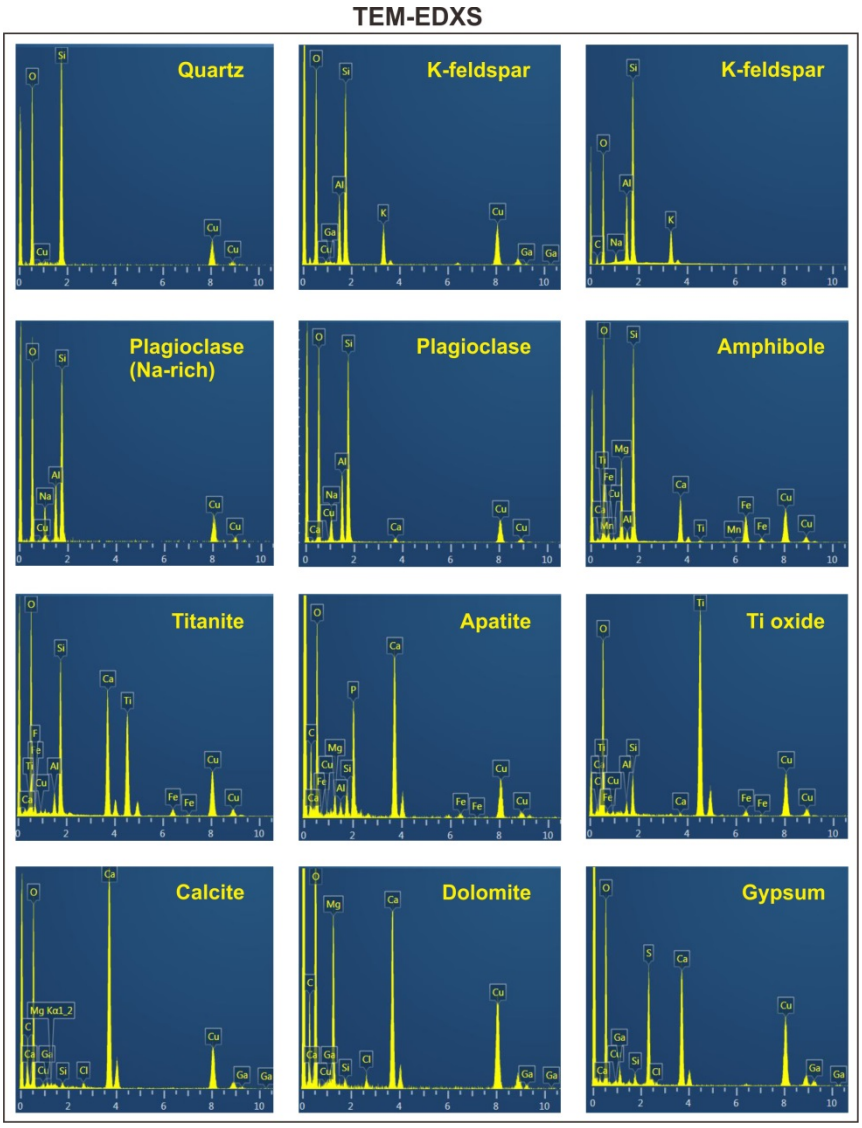

Fig. S1. TEM EDXS patterns of constituent minerals of dust particles obtained from the cross-sectional slices prepared by FIB.

TEM identification of phyllosilicate minerals

Phyllosilicate minerals were abundant in the mineral dust. The identification of muscovite, biotite, and chlorite was rather straightforward from their characteristic chemical compositions with the aid of lattice-fringe imaging (Fig. S2). However, the identification of nano-thin phyllosilicates (clay minerals) was difficult because of their breakdown under electron beam and small grain size below the minimum diameter of electron beam for EDXS. They occurred often as agglomerates. In addition, mixed layering of illite and smectite is common in natural soils. The identification of clay minerals was based on lattice fringes and chemical compositions: 1.0 nm for illite, ~1.0 nm for smectite and vermiculite, and ~7.0 nm for kaolinite (Fig. S2). Kaolinite was directly identified from its EDXS with the aid of lattice fringe imaging. However, illite, smectite, and illite-smectite mixed layers could not be separately identified each other because smectite was contracted under the high vacuum of the TEM chamber, showing ~1.0 nm lattice fringes similar to those of illite. Although EDXS can be used for identifying illite and smectite with interlayer cations K and Ca, respectively, they cannot be separately analyzed using EDXS, even when using an electron beam as small as possible. Therefore, we could not distinguish between nano-thin illite, smectite, and their mixed-layers, using conventional TEM work. To avoid over-interpretation, nano-thin platelets of clay minerals showing ~1.0 nm lattice fringes with varying K and Ca contents were grouped into illite-smectite series clay minerals (ISCMs). ISCMs are nano-scale mixtures of nano-thin platelets of illite, smectite, and illite-smectite mixed-layers.

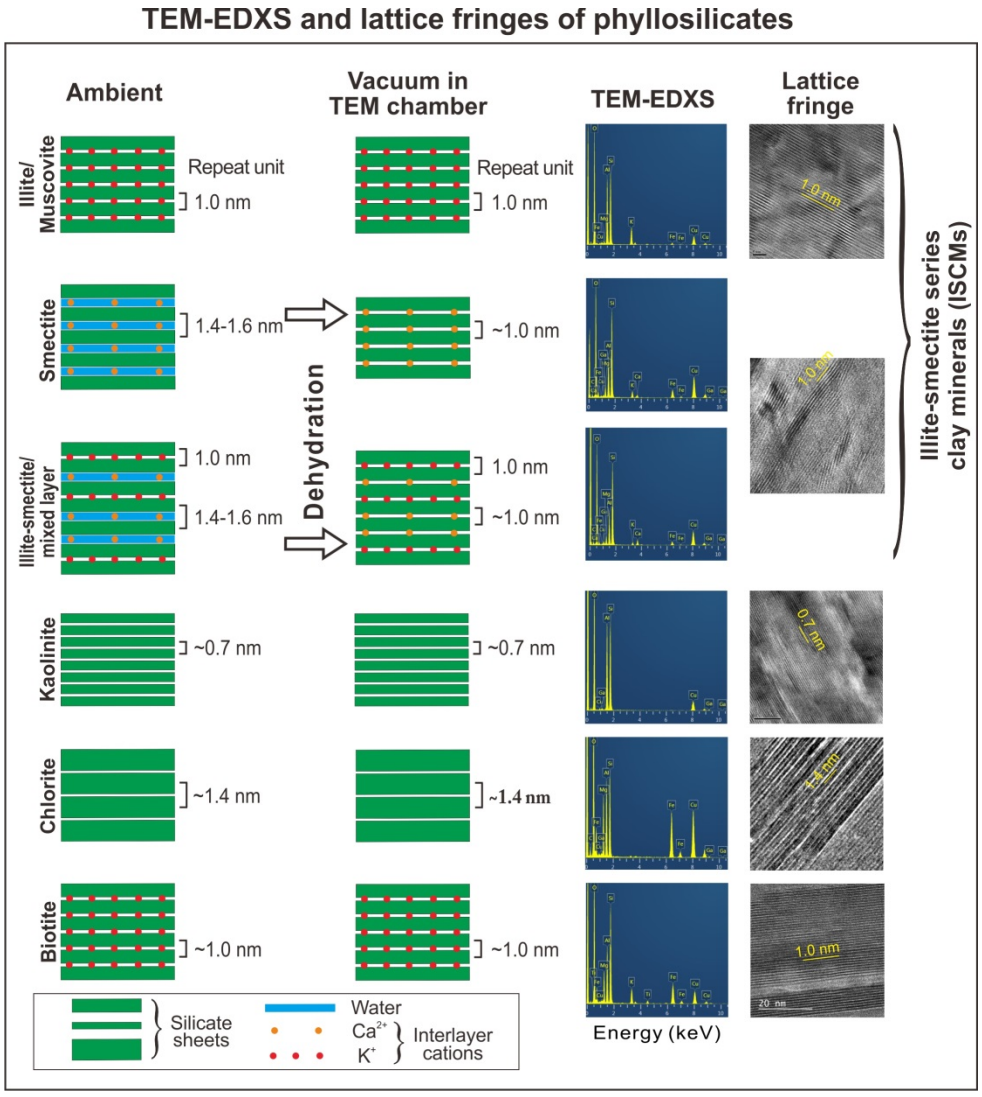

Fig. S2. Identification of phyllosilicates using TEM-EDXS and lattice fringes.

TEM identification of iron (hydr)oxides

Mineralogical identification of iron (hydr)oxides was also challenging. EDXS could not be used for the identification. Electron diffraction and lattice-fringe imaging should be used in combination as shown in Fig. S3. However, many iron (hydr)oxide grains could not be identified because of the overlap of many *d*-spacings, varying crystallographic orientation, and tiny grain sizes. Thus, we used species names only in cases in which mineral species were identified unambiguously by lattice fringe imaging and electron diffraction; in other cases, we used the collective term "iron (hydr)oxide".

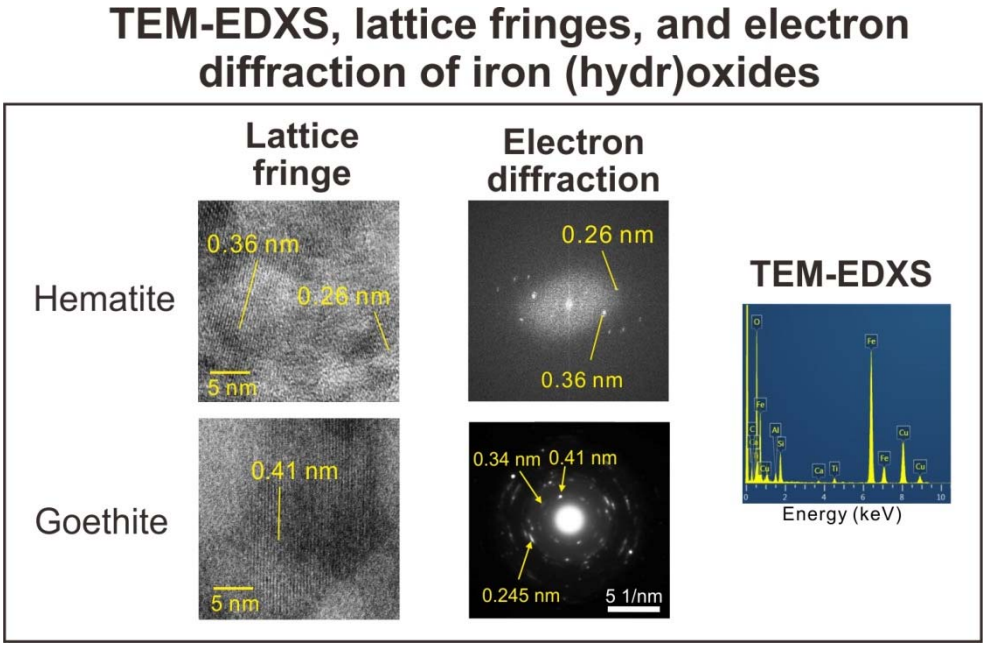

Fig. S3. Identification of phyllosilicates using lattice fringes and electron diffraction.

Mineralogical classification of dust particles using SEM-EDXS

Dust particles are essentially mixtures of mineral grains of diverse species and sizes. In case the quantity of powder dust samples is sufficient (~several hundred mg), XRD method is best for the determination of mineral composition. SEM-EDXS analyses of individual particle can be used when powder samples are insufficient or non-available. Ideally, mineral composition of individual dust particle can be determined by mixing several minerals to get the overall chemical composition of the particle. Then, the summation of the mineral compositions of thousands of dust particles considering their volume would lead to the mineral composition of bulk dust. However, the irregular morphology of dust particles prohibits the accurate determination of dust particles due to the difficulty of calibration. In addition, the chemical compositions of constituent minerals are varied. Prior to the development of reliable quantitative analysis procedure based on SEM for the mineral composition of individual dust particle, we adopted semi-quantitative approach. Since dust particles are generally dominated by one mineral species or group, we have determined the predominant mineral of a dust particle referring to the EDXS patterns of pure minerals as shown in Figs. S1 and S2. In case particles show intermediate EDXS pattern (Fig. S4), half of the particle was counted (0.5). Summation of the counts led to the approximate mineral composition of bulk dust. Although the procedure is evidently semi-quantitative, SEM-EDXS results were consistent with XRD results in the recent analyses of Asian dust (Table 1 in Park and Jeong (2016), Journal of the Mineralogical Society of Korea, 29, 79–87).

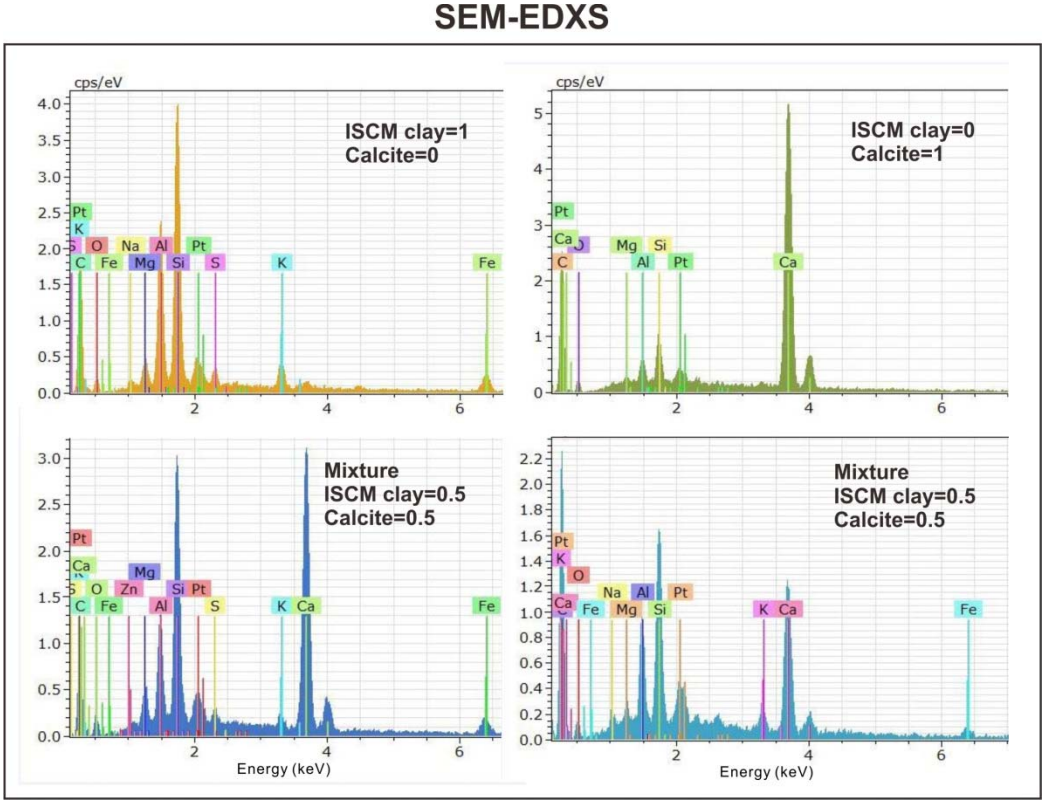

Fig. S4. SEM-EDXS of dust particles.

Park and Jeong (2016)

Table 1. Mineral compositions of Asian dusts determined by XRD analysis and SEM-EDS single particle analysis

Minerals	Asian dust XRD				
	Feb 22 2015	Mar 18 2014	Mar 31 2012	Mar 20 2010	Average
	(This study)	(Jeong and Achterberg, 2014)			
ISCMs	55	60	42	50	51
Kaolinite	2	1	3	4	3
Chlorite	5	3	6	7	5
Total clay	*62*	*64*	*52*	*61*	59
Quartz	18	14	23	15	17
Plagioclase	10	11	15	10	12
K-feldspar	4	0	6	2	3
Amphibole	0	0	1	2	1
Calcite	5	5	2	5	4
Gypsum	1	6	2	6	4
Total	100	100	100	100	100
	SEM single particle analysis				
ISCMs	57	54	48	54	52
Kaolinite	2	1	3	2	2
Chlorite	3	2	4	6	4
Total clay	*62*	*58*	*55*	*62*	58
Quartz	19	19	21	17	19
Plagioclase	9	11	11	10	11
K-feldspar	3	4	5	3	4
Amphibole	0	1	1	0	1
Calcite	4	7	7	6	7
Gypsum	2	0	1	1	1
Total	100	100	100	100	100

We will prepare final version considering comment and reply above.

Sincerely

On behalf of co-authors

Gi Young Jeong
Corresponding Author